ELSEVIER

Journal of Alloys and Compounds 404–406 (2005) 743–747

Journal of ALLOYS AND COMPOUNDS

www.elsevier.com/locate/jallcom

Isothermal decomposition of $LiAlD_4$ with and without additives

D. Blanchard[a,*], H.W. Brinks[a], B.C. Hauback[a], P. Norby[b], J. Muller[a]

[a] *Institute for Energy Technology, P.O. Box 40, NO-2027, Kjeller, Norway*
[b] *University of Oslo, P.O. Box 1033, NO-0315 Blindern, Oslo, Norway*

Received 9 September 2004; accepted 20 January 2005
Available online 19 July 2005

Abstract

The isothermal decompositions of pure $LiAlD_4$ and $LiAlD_4$ ball-milled with VCl_3 and $TiCl_3 \cdot (1/3)(AlCl_3)$ have been studied by synchrotron X-ray diffraction. The changes of the different phases are examined during the decomposition and the activation energies and kinetics parameters are derived. Two periods of decomposition are observed. The first is an induction period governed by the nucleation of new phases. The second is the main decomposition period where the apparent activation energies and the kinetics are affected by the additives. VCl_3 appears to be a better additive in regard of decreasing the apparent activation energy and enhancing the kinetics of the decomposition.

Keywords: Hydrogen storage; Lithium aluminium hydride; Alanate; Ball-milling

1. Introduction

In order to develop high gravimetric capacity hydrogen storage units for mobile applications, the alanates appear to be one of the most promising hydrogen storage materials to fulfil the requirements, e.g. by the International Energy Agency (working temperature 80–100 °C, capacity more than 5 wt% hydrogen). Among these compounds, lithium aluminium hydride, $LiAlH_4$, is very attractive with a total hydrogen content of 10.6 wt% of hydrogen in total, and 7.9 wt% being accessible at temperatures below 250 °C [1]. Upon heating, hydrogen is released in a three-steps decomposition reaction [2,3]:

$$3LiAlH_4 \rightarrow Li_3AlH_6 + 2Al + 3H_2$$
$$(5.2\,\text{wt\% H},\ T \approx 160\,^\circ\text{C}) \quad (1)$$

$$Li_3AlH_6 \rightarrow 3LiH + Al + (3/2)H_2$$
$$(2.6\,\text{wt\% H},\ T \approx 210\,^\circ\text{C}) \quad (2)$$

$$3LiH + 3Al \rightarrow 3LiAl + (3/2)H_2$$
$$(2.6\,\text{wt\% H},\ T \approx 400\,^\circ\text{C}) \quad (3)$$

The last decomposition step occurs at too high temperature to be considered as accessible for practical purpose.

A breakthrough for the possible use of alanates as a hydrogen storage material was achieved by the successful catalysis of $NaAlH_4$ with Ti-compounds giving reversible hydrogenation, enhanced kinetics and lowered desorption temperatures [4]. Several studies have been carried out for $LiAlH_4$ with solid-sate additives introduced by ball-milling. $TiCl_3 \cdot (1/3)(AlCl_3)$ [5,6], $TiCl_4$, TiH_2 and Al_3Ti_5 [7] or VCl_3 [6] as additives, the first and second decomposition temperatures are decreased by 50–60 and 20–25 °C, respectively. The best results are obtained with VCl_3. However, the pressure needed for absorption of hydrogen in the $LiAlH_4$ system is currently not known.

The origins of the desorption kinetics enhancement and the reduced decomposition temperatures are not understood. Detailed studies of the desorption and absorption processes in alanates with different additives are needed to improve the understanding of the involved mechanisms. In the present study, isothermal decomposition of pure $LiAlD_4$ and $LiAlD_4$

* Corresponding author. Tel.: +47 63 80 60 67; fax: +47 63 81 09 20.
E-mail address: didier.blanchard@ife.no (D. Blanchard).

0925-8388/$ – see front matter © 2005 Elsevier B.V. All rights reserved.
doi:10.1016/j.jallcom.2005.01.126

ball-milled with two different additives, VCl_3 and $TiCl_3 \cdot (1/3)(AlCl_3)$, has been investigated by in-situ synchrotron powder X-ray diffraction (PXD).

2. Experimental

The compounds, $LiAlD_4$ (≥95% purity, containing ~0.2 mol% LiCl), $TiCl_3 \cdot (1/3)(AlCl_3)$ (99.99%) and VCl_3 (99.99%) were purchased from Sigma–Aldrich. All sample handling was carried out in glove box in a dry argon atmosphere. Typically, 1.0 g of $LiAlD_4$ was ball-milled for 5 min in a Pulverisette 7 planetary ball mill at a gyration rate of 400 rpm. Hardened steel vial of 12 cm^3 sealed under argon with three steel balls (7 g each) were used.

In situ PXD data were collected at the Swiss–Norwegian beam line (station BM1A) at the European Radiation Source Facility (ESRF) in Grenoble, France. A capillary-based cell, 0.5 mm in diameter, that allowed collection of PXD data during heating by a hot air blower under dynamical vacuum, was used. The sample was contained in a boron–silica-glass capillary and kept in place by a glass needle. The sample was placed under the air blower once the set temperature was reached. An imaging plate system (MAR 345) was used to collect two-dimensional powder diffraction patterns with exposure times of 30 s. Data were collected every second minute (owing to the read and erase time for the image plate). The wavelength was 0.7100 Å. The data range was 3–34° in 2θ and rebinned with a step size of 0.015°. The program Fit2D [8] was used to reduce the raw data to one-dimensional PXD patterns.

Rietveld refinements were carried out using the program Rietica [9]. Structural data for $LiAlD_4$ and Li_3AlD_6 were taken from [10,11], respectively. Voigt profile functions were used, and the background was modelled by Cheby II polynomials.

The isothermal decomposition of (i) pure $LiAlD_4$, (ii) $LiAlD_4$ with 2 mol% VCl_3, and (iii) $LiAlD_4$ with 2 mol% $TiCl_3 \cdot (1/3)(AlCl_3)$ were studied at different temperatures. Diffraction diagrams were collected for the sample without additives at: 154, 156, 163, 167 °C and for the two samples with additives at: 139, 148, 152 and 156 °C, respectively.

3. Results and discussion

Fig. 1 shows the complete set of PXD patterns measured during the decomposition of $LiAlD_4$ + 2 mol% VCl_3 at 156 °C. The decomposition (Eq. (1)) of $LiAlD_4$ into Li_3AlD_6 and Al can easily be followed. Different samples, pure lithium alanate or ball milled with $TiCl_3 \cdot (1/3)(AlCl_3)$ or VCl_3 additives, gave similar patterns.

Rietveld refinements of the diffraction data were used to determine the composition of each sample, and thereby the crystalline volume fraction, φ_c, of each crystalline phase during the thermal decomposition. Information about the kinetics of the decomposition can be found from a linear fit of $\ln[-\ln(1-\varphi_c)]$ plotted versus ln(t) according to the Avrami equation [12]:

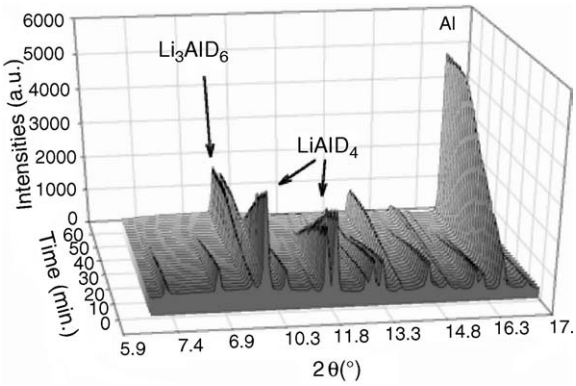

Fig. 1. The PXD patterns during the isothermal decomposition at 156 °C of $LiAlD_4$ with 2 mol% VCl_3.

$$\varphi_c = 1 - \exp(-(kt)^n) \quad (4)$$

where k represents the rate of the reaction and t is the time during the decomposition.

3.1. The changes in phase compositions

Fig. 2 shows the evolution of the crystalline volume fractions during the isothermal decomposition of pure $LiAlD_4$ and $LiAlD_4$ with 2 mol% VCl_3 or 2 mol% $TiCl_3 \cdot (1/3)(AlCl_3)$ additives. It is important to notice that at $t = 0$ the samples composition are different between pure and samples with additives. During ball milling some of the $LiAlD_4$ is decomposed to Al, LiCl and Li_3AlD_6because of the additives reduction as well as its thermal decomposition [6,13]. This effect is more pronounced for the $TiCl_3 \cdot (1/3)(AlCl_3)$ additive than for VCl_3 (Fig. 2b). When the first step decomposition is finished, the amount of Al is always larger than expected from the stoichiometry from Eq. (1). Despite the low temperatures (<167 °C) some thermal decomposition of Li_3AlD_6 occurs (Eq. (2)). This second decomposition is rather important for the samples with additives; the kinetic of reaction describes by Eq. (2) is increased at a given temperature by using V- and Ti-based additives [6].

The plots for the crystalline volume fraction evolution of pure $LiAlD_4$ and $LiAlD_4$ with 2 mol% VCl_3, during the decomposition (Fig. 2a and c) show sigmoid shapes. Three different regions are clearly present and interpreted: (i) an induction period with a slow decomposition rate; (ii) a main decomposition with a constant rate of decomposition; finally (iii) a reduced decomposition rate until $LiAlD_4$ disappears.

3.2. The Avrami plots

Fig. 3 shows the logarithm of the Avrami equation for two different samples: pure $LiAlD_4$ and $LiAlD_4$ with 2 mol% VCl_3 decomposed at 156 °C. The plots clearly indicate two

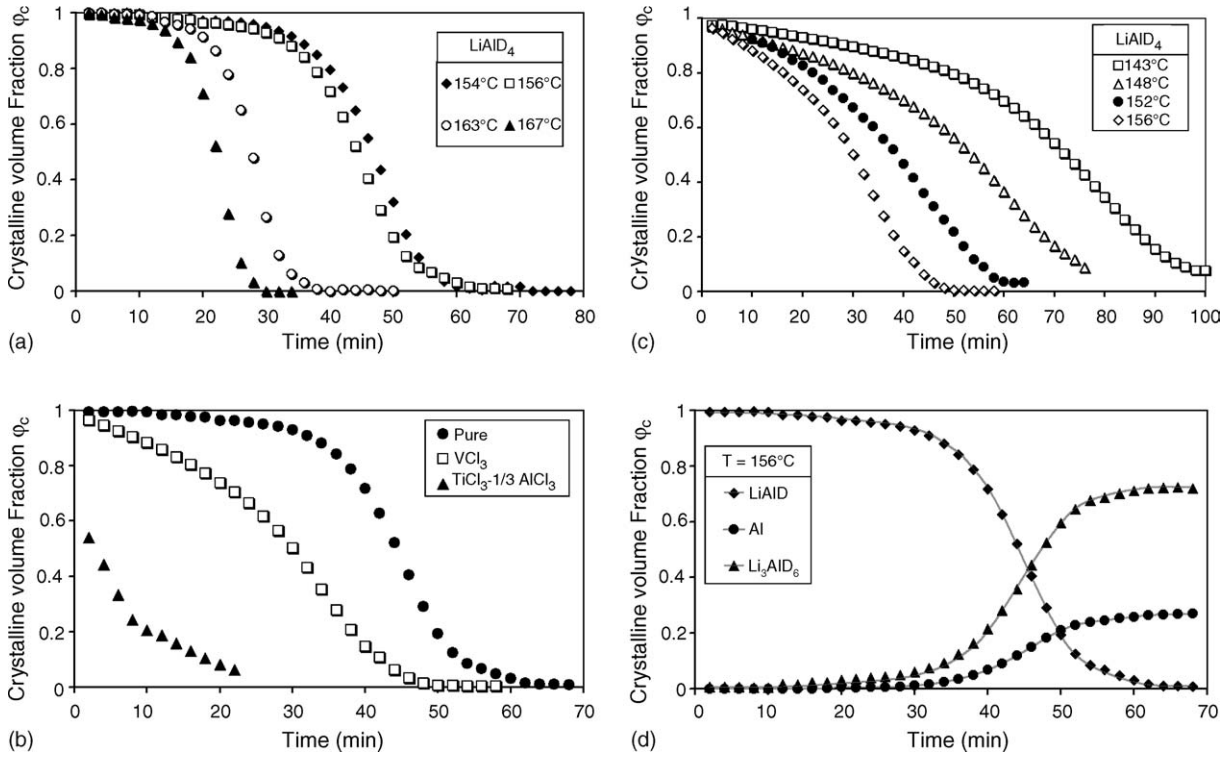

Fig. 2. Changes in the volume fraction of $LiAlD_4$ during the decomposition: (a) pure $LiAlD_4$ at 154, 156, 163 and 167 °C; (b) Comparison between pure $LiAlD_4$ and $LiAlD_4$ with 2 mol% VCl_3 and 2 mol% $TiCl_3 \cdot (1/3)(AlCl_3)$ at 156 °C; (c) $LiAlD_4$ with 2 mol% VCl_3 at 143, 148, 152 and 156 °C; (d) volume fractions of $LiAlD_4$, Li_3AlD_6 and Al for the pure sample at 156 °C.

separate regions covering the induction and the main decomposition period. This result may indicate that the two first periods are not driven by the same mechanisms of decomposition.

3.3. The induction period

The induction period indicates that the beginning of the decomposition is governed by a slow production rate of Al or Li_3AlD_6 nucleus [14]. When the nuclei size or concentration has reached a certain level, the rate of the reaction increases. It is difficult to establish here if the decomposition is controlled by the nucleation itself or by the diffusion of the species or the interface process.

This period is shortened or even not observed at all when the samples are mixed with additives. Indeed some nucleation has already been achieved during the ball milling. The induction period is not observed for $LiAlD_4$ with 2 mol% $TiCl_3 \cdot (1/3)(AlCl_3)$. The sample already contains a significant amount of Li_3AlD_6 and Al after the ball-milling, and the phase composition at $t = 0$ is: $LiAlD_4 \sim 40$ mol%, $Li_3AlD_6 \sim 43$ mol%, Al ~13 mol% and LiCl ~ 4 mol% (Fig. 2b).

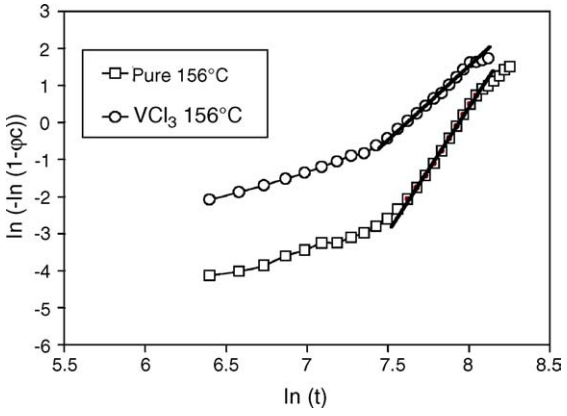

Fig. 3. Logarithmic form of the Avrami equation during the whole decomposition for pure $LiAlD_4$ and $LiAlD_4$ with 2 mol% VCl_3 decomposed at 156 °C.

3.4. The main decomposition

After the induction period the rate of decomposition rapidly increases to reach a constant value. Fig. 4 shows the Avrami plots for this period for pure $LiAlD_4$ and $LiAlD_4$ with VCl_3 decomposed at different temperatures. The k values are determined using the best-fitted lines. The rate of decomposition depends on the temperature, and can be described by the familiar Arrhenius-type equation [15]:

$$k = A\,e^{-E_a/RT} \quad (5)$$

where A is the temperature independent frequency factor, E_a contains both the overall free energy change for the formation

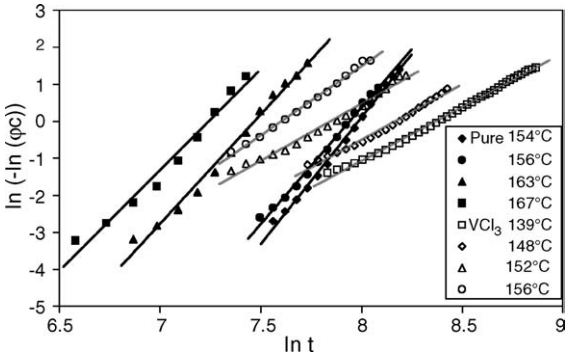

Fig. 4. Logarithmic form of the Avrami equation during the main decomposition period for pure $LiAlD_4$ and $LiAlD_4$ with 2 mol% VCl_3.

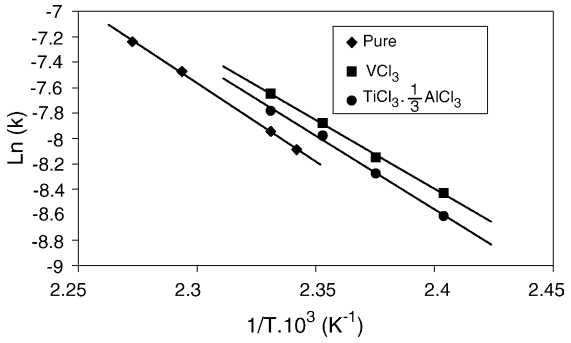

Fig. 5. $\ln k$ vs. $1/T$ in K for pure $LiAlD_4$, $LiAlD_4$ ball milled with 2 mol% VCl_3 and 2 mol% $TiCl_3 \cdot (1/3)(AlCl_3)$ during the bulk decomposition.

of a nucleus and the activation energy for short-range diffusion of the atoms, R the gas constant and T is the absolute temperature. The natural logarithm of the k values versus $1/T$ (Arrhenius-type plot) is shown in Fig. 5 for the three $LiAlD_4$ samples.

The derived apparent activation energies, E_a, are 102, 95, 90 kJ/mol for pure $LiAlD_4$, $LiAlD_4$ with 2 mol% $TiCl_3 \cdot (1/3)(AlCl_3)$ and with 2 mol% VCl_3, respectively. These values are higher than the activation energy of 42.6 kJ/mol published for $LiAlH_4$ with 2 mol% $TiCl_3 \cdot (1/3)(AlCl_3)$ [5]. This result was obtained by volume measurements of H_2 release using a Sieverts-type apparatus. The E_a values are consistent relating the desorption temperatures for $LiAlD_4$ with and without additives. The decomposition temperature is lower with VCl_3 than with $TiCl_3 \cdot (1/3)(AlCl_3)$ additives [6]. Furthermore, $E_{a\,LiAlD_4} > E_{a\,LiAlD_4+TiCl_3\cdot(1/3)(AlCl_3)} > E_{a\,LiAlD_4+VCl_3}$ indicates that the rates of decomposition are less temperature dependent when additives have been used. Finally it is found that the decomposition rates are enhanced with additives. At 156 °C, $k_{VCl_3} \sim 1.15 k_{TiCl_3\cdot(1/3)(AlCl_3)} \sim 1.20 k_{pure}$, indicating that the rates of decomposition are larger with VCl_3 additive.

4. Conclusions

The first decomposition reaction (Eq. (1)) of pure $LiAlD_4$ and $LiAlD_4$ with 2 mol% VCl_3 or $TiCl_3 \cdot (1/3)(AlCl_3)$ have been studied by in-situ synchrotron X-ray diffraction under dynamical vacuum at isothermal conditions. Rietveld refinements of each diffraction pattern have been used to determine the crystalline volume fractions for each phase during the isothermal decompositions.

For the pure $LiAlD_4$ and $LiAlD_4$ with V-based additives, the decompositions consist of an induction period followed by a main decomposition. Avrami plots indicate that the two first periods do not follow the same route of decomposition. The induction period may correspond to the time needed to obtain the first clusters of Al or Li_3AlD_6. Its duration, and thereby the whole decomposition period, is affected by the presences of Al or Li_3AlD_6 prior to the decomposition. This observation can help to find a strategy to enhance the kinetics of alanates. Available seeds for nucleation are important to decrease the duration of the decomposition.

During the main decomposition, the apparent activation energies differ for the different additives. They are correlated with the decomposition temperatures and rates. Summing up, the activation energies (E_a), the decomposition temperatures and the inverse of the decomposition rates ($1/k$), can be ranked in the following sequence: pure $LiAlD_4 > LiAlD_4 + 2\,mol\%\,TiCl_3 \cdot (1/3)(AlCl_3) > LiAlD_4 + 2\,mol\%VCl_3$.

Acknowledgements

The skilful assistance from the project team at the Swiss Norwegian Beam Line at ESRF is gratefully acknowledged. The work has received financial support from the Marie Curie projects ENK6-CT-2002-50519 and ENK6-CT-2002-00600 (“HYSTORY”) under the 5FP EESD program in the European Commission.

References

[1] T.N. Dymova, D.P. Aleksandrov, V.N. Konoplev, T.A. Silina, A.S. Sizareva, Russ. J. Chem. 20 (1994) 263.
[2] V. Mikheeva, S. Arkhipov, Zh. Neorg. Khim. 12 (1967) 2025.
[3] T.N. Dymova, D.P. Aleksandrov, V.N. Konoplev, T.A. Silina, Koord. Khim. 20 (1995) 175.
[4] B. Bogdanovic, M. Schwickardi, J. Alloys Compd. 253–254 (1997) 1.
[5] J. Chen, N. Kuriyama, Q. Xu, T.H. Takeshita, T. Sakai, J. Phys. Chem. B 105 (2001) 11214.
[6] D. Blanchard, H.W. Brinks, B.C. Hauback, P. Norby, MatER. Sci. Eng. B108 (2004) 54.
[7] V.P. Balema, J.W. Wiench, K.W. Dennis, M. Pruski, V.K. Pecharsky, J. Alloys Compd. 329 (2001) 108.
[8] A.P. Hammersley, S.O. Svensson, M. Hanfland, A.N. Fitch, D. Häusermann, High Pressure Res. 14 (1996) 235.
[9] B. Hunter, Commission For Powder Diffraction, Int. Union of Crystallography, Newsletter No. 20, 1998.
[10] B.C. Hauback, H.W. Brinks, H. Fjellvåg, J. Alloys Compd. 346 (2002) 184.
[11] H.W. Brinks, B.C. Hauback, J. Alloys Compd. 354 (2003) 143.

[12] R.J. Borg, G.J. Dienes, The Physical Chemistry of Solids, Academic Press Inc., Boston, 1992.
[13] V.P. Balema, K.W. Dennis, V.K. Pecharsky, Chem. Commun. (2000) 1665.
[14] W.E. Garner, E.W. Haycock, Proc. Koy. Soc. 211A (1952) 351.
[15] Z.D. Jastrzebski, The Nature and Properties of Engineering Materials, John Wiley and Sons, New York, 1987.